

Plasma Dynamics in Capillary Discharge Soft X-Ray Lasers

A. Ben-Kish,¹ M. Shuker,¹ R. A. Nemirovsky,¹ A. Fisher,¹ A. Ron,¹ and J. L. Schwob²

¹*Department of Physics, Technion-Israel Institute of Technology, Haifa 32000, Israel*

²*Racach Institute of Physics, The Hebrew University, Jerusalem 91904, Israel*

(Received 30 November 2000; published 18 June 2001)

The dynamics and stability of collapsing gas columns, generated by a fast capillary discharge setup, are studied for obtaining soft x-ray amplification in highly ionized ions. Electron temperature and density measurements at the peak of the compression stage are used for tuning the discharge parameters. Once the needed conditions were achieved, strong amplification of the $3s-3p$ transition in Ne-like Ar ions at 469 \AA is observed. A gain coefficient of $>0.75 \text{ cm}^{-1}$ and a beam divergence of $<5 \text{ mrad}$ are measured along plasma columns of $<150 \text{ }\mu\text{m}$ diameter and up to 165 mm length.

DOI: 10.1103/PhysRevLett.87.015002

PACS numbers: 52.59.Ye, 42.55.Vc, 52.50.Lp, 52.70.La

Soft x-ray lasers were first demonstrated by Matthews *et al.* [1] and by Suckewer *et al.* [2]. In the Ne-like ions scheme [1] a powerful laser was used to produce a Ne-like Se (Se^{24+}) plasma column and to induce soft x-ray amplification at 206 \AA . In recent work conducted by Rocca *et al.* [3,4] amplification of soft x-ray radiation in Ne-like Ar and S was obtained by a fast capillary discharge. In this more efficient scheme a current pulse is injected into a gas column confined in a capillary tube. The current induces a fast radial collapse towards the axis, producing a shock wave that heats the plasma column. Under certain plasma conditions [5,6] soft x-ray amplification along the axis is obtained. Stable and uniform plasma column collapse is crucial in this scheme. Furthermore, specific plasma conditions in the compressed column must be obtained simultaneously. For example, in the Ne-like Ar amplifier these include [5,6] high abundance of Ar^{8+} ions, specific electron density ($\sim 10^{19} \text{ cm}^{-3}$) and temperature ($\sim 60 \text{ eV}$), suitable electron density profile, and small transverse column dimensions.

In this Letter we discuss new methods for investigating the dynamics and stability of collapsing gas columns in a capillary discharge setup. Furthermore, we use time-resolved soft x-ray spectroscopy to determine the plasma conditions in the column core. By applying these techniques and comparing the results to numerical simulations, we demonstrate a methodical way to achieve the conditions for soft x-ray amplification in a capillary discharge experiment. In the last part of this Letter we describe the basic properties of the Ne-like Ar laser produced in our laboratory.

Our fast capillary discharge setup [7,8] consists of a 1 MV , $7 \text{ }\Omega$ transmission line driving an Ar filled capillary tube ($0.3\text{--}1 \text{ Torr}$ Ar, $80\text{--}180 \text{ mm}$ length, $4\text{--}5 \text{ mm}$ inner diameter). A prepulse is applied to the Ar gas ($4\text{--}20 \text{ }\mu\text{s}$, $5\text{--}100 \text{ A}$) through a coil wound around the capillary tube, followed by a main current pulse (sine-like shape, $t_{1/4} = 51 \text{ ns}$, $I_{\text{max}} = 35\text{--}65 \text{ kA}$). To ensure the breakdown of the gas load a small spark was triggered prior to the prepulse. The collapse toward the center of the capillary heats the gas to about 100 eV , inducing soft x-ray

emission. A 3 mm hole drilled in the anode allows the soft x-ray radiation to escape towards the detection system. The detection system consists of a gated ($2\text{--}5 \text{ ns}$) off-axis pinhole camera [9], a Schwob-Fraenkel soft x-ray spectrometer [10] with similar gating capabilities, and x-ray photodiodes with various cathodes.

In order to achieve soft x-ray lasing in this scheme the radial collapse of the plasma column must be stable. It was found that the prepulse has a major influence on the stability of the column. While certain prepulse conditions allow for a stable compression, inadequate conditions produce, in most of the cases, a nonuniform column [7]. Furthermore, shots with no prepulse at all resulted in breakdowns outside the capillary and destruction of the capillary holder.

Soft x-ray imaging of the source is used, in this work, for investigating the stability of the plasma column. Because of the opacity of the capillary tube imaging perpendicular to the column is impossible; therefore, an off-axis pinhole camera was used. This camera consists of a four-pinhole array placed 50 mm from the capillary tip. The $60 \text{ }\mu\text{m}$ diameter holes were placed 1.7 mm off the axis of the capillary, forming a square. Using this setup, images of the column from four directions were obtained at a viewing angle of $\sim 1.5^\circ$ (see Fig. 1). This angle allows imaging of the entire length of the plasma column (80 mm in this case) through the 3 mm hole in the anode [9]. The images

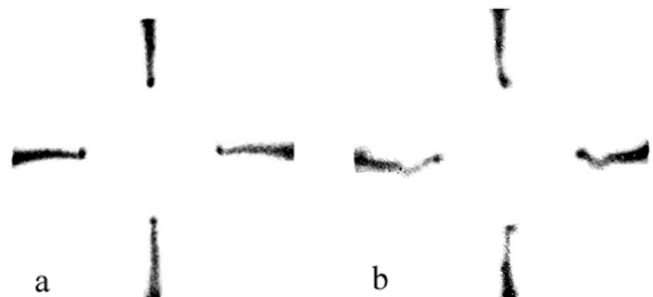


FIG. 1. Images of the hot plasma core ($R \sim 75 \text{ }\mu\text{m}$) in stable (a) and nonstable (b) compression conditions, imaged from four directions at a viewing angle of $\sim 1.5^\circ$.

were recorded on a gated microchannel plate (MCP) camera placed 370 mm from the pinholes. A $2\ \mu\text{m}$ Mylar filter was placed in front of the camera limiting its spectral response to the $43.6\text{--}65\ \text{\AA}$ range. A detailed soft x-ray spectroscopic analysis of the capillary source emission [11] confirmed that the emitted radiation in this spectral range originates only from $2p\text{--}3s$ Ne-like and $2p\text{--}3s$ F-like Ar (Ar^{8+} , Ar^{9+}) line emission. Accordingly, the images reflect the size of the plasma column in which the relevant ions for the soft x-ray laser action exist.

The influence of the prepulse on the compression stability is demonstrated in Fig. 1. Two sets of soft x-ray images of plasma columns are shown, obtained by using a 4.2 mm diameter, 80 mm long capillary tube filled with an initial Ar pressure of 500 mT. In both cases, the images were recorded 40 ns after the onset of the main current pulse ($t_{1/4} = 51\ \text{ns}$, $I_{\text{max}} = 40\ \text{kA}$), when the converging shock wave reaches the capillary axis. The measured column radius at this stage is $75\ \mu\text{m}$. In the first experiment [Fig. 1(a)] a 50 A amplitude prepulse was triggered $10\ \mu\text{s}$ before the main pulse onset. In the second experiment [Fig. 1(b)] the prepulse amplitude was only 5 A. As can be seen from the images, the 50 A prepulse induces a stable radial collapse while the 5 A prepulse results in an unstable compression. A geometrical ray-tracing code showed that a 10 mm segment in the center of the plasma column is shifted $\sim 150\ \mu\text{m}$ from the axis. It is clearly evident that the plasma conditions in this case [Fig. 1(b)] are not suitable for achieving lasing. According to our measurements, prepulse currents above 10 A are needed for obtaining a stable collapse in every experiment. However, prepulse currents significantly higher than 50 A may change the initial temperature and pressure in the plasma and consequently change the dynamics of the collapse.

After the appropriate prepulse conditions were determined, the off-axis pinhole setup was used to investigate the dynamics of the plasma column. Four pinhole images of the plasma column taken 39.5, 44, 52, and 56 ns after the onset of the current pulse, are presented in Fig. 2(a). The diameter of the plasma along the column, at each measured time, can be deduced from the pinhole images, while taking into account the different magnification along the axis (this effect causes the conical shape of the plasma column in the pinhole images). It was found that when the radial collapse is stable the diameter of the measured plasma along the column is uniform.

The four images in Fig. 2(a) were taken through the $2\ \mu\text{m}$ Mylar filter, limiting the spectral response to only Ar^{8+} and Ar^{9+} lines. These images show an expansion of the hot region in the plasma. We attribute this expansion to the reflection of the converging shock wave that reaches the axis, expands, and heats the column's core. We note that before the arrival of the shock wave to the axis no radiation of F-like or Ne-like Ar ions is detected. This fact demonstrates the dominant role of the shock wave in heating the plasma in the capillary discharge scheme. Further-

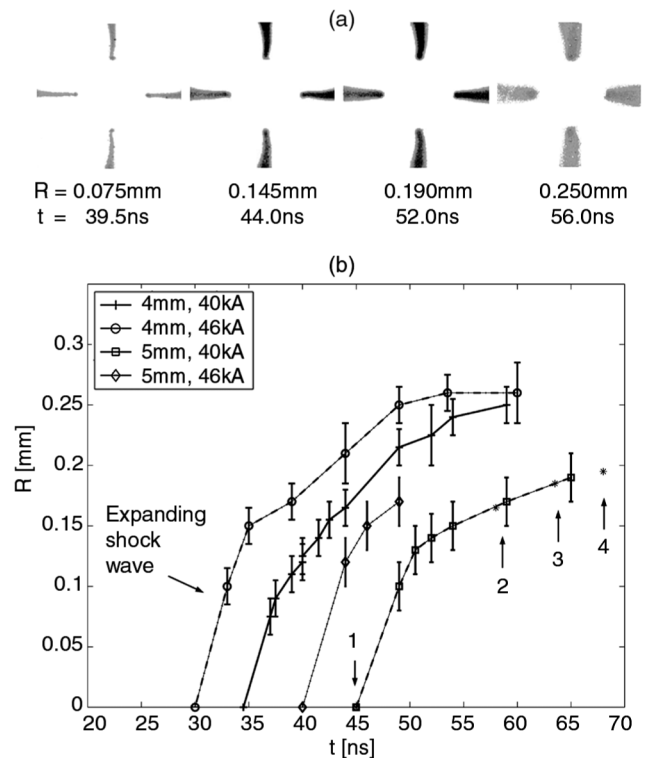


FIG. 2. (a) Images of the hot plasma region (Ar^{9+} , Ar^{8+} ions) during the expansion phase ($I_{\text{max}} = 40\ \text{kA}$, $D = 4.2\ \text{mm}$). (b) The measured hot region radius vs time in four setups ($I_{\text{max}} = 40, 46\ \text{kA}$, $D = 4, 5\ \text{mm}$). The four arrows at the right-hand side indicate the times at which the spectra in Fig. 3 were obtained.

more, the observation of significant radiation flux in this spectral window ($43.6\text{--}65\ \text{\AA}$) indicates that the plasma is heated to the relevant electron temperature for the Ne-like Ar laser experiment.

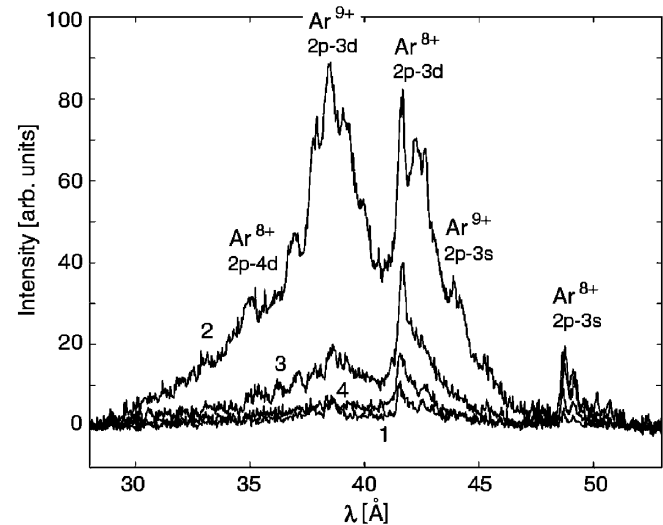


FIG. 3. Soft x-ray spectra in the $25\text{--}50\ \text{\AA}$ range (3 ns exposure time). The spectra were taken at the times and radii indicated in Fig. 2(b) by small arrows (1–4) near the 40 kA–5 mm expansion graph.

Using the off-axis camera apparatus the expanding hot region radius as a function of time was measured in four sets of experiments [Fig. 2(b)] utilizing different capillary diameters (4 and 5 mm) and different current amplitudes (40 and 46 kA). In all cases the plasma core shows a rapid expansion caused by the reflected shock wave ($V_{\text{shock}} \sim 40$ km/s) followed by a more moderate growth ($\sim 1/4 V_{\text{shock}}$) due to the radial velocity of the plasma particles.

The measurements presented in Fig. 2 reveal the basic dynamics of the formation of a high temperature plasma column in the peak of the capillary discharge process. However, determining the suitable external parameters (e.g., current pulse, capillary diameter, gas pressure) in order to achieve lasing along the column demands a more detailed measurement of the plasma properties. Specifically, time-resolved measurements of the Ne-like ions abundance, as well as electron temperature and density measurements, are of prime importance. For this purpose time-resolved (3 ns shutter time) soft x-ray spectroscopic measurements were used. A 2 m Schwob-Fraenkel spectrometer [10], equipped with a 600 l/mm grating and a 21 μm slit, was adjusted to the spectral range of 25–50 \AA . This spectral range was chosen due to the existence of resonance transitions to the ground state of the Ne-like and F-like Ar ions (Ar^{8+} , Ar^{9+}) in this region, including the optical deexcitation transition $2p-3s$ that governs the depletion of the lower level of the Ne-like Ar laser transition.

From the time-resolved spectrum in this region, rather than in the lasing region, the relevant plasma properties can be inferred. Several spectra were taken at different initial pressures, capillary dimensions, capillary materials, and main current intensities. An example set of measurements, using near optimal parameters, is shown in Fig. 3 demonstrating the different stages of the expansion. In this case a 5 mm inner diameter, 80 mm long capillary filled with 500 mTorr of Ar gas, was used. The main current amplitude was 40 kA and a 1 kGauss longitudinal magnetic field was applied. The spectra in Fig. 3 correspond to the times 45, 58, 64, and 68 ns after the onset of the current [the diameter of the hot region at these different times is indicated in Fig. 2(b) by small arrows on the 40 kA–5 mm column expansion graph]. One can notice a qualitative change in the spectrum structure taken at different times. For example, while in spectrum No. 2 the intensity of the Ar^{8+} and Ar^{9+} $2p-3d$ lines is similar; in spectra Nos. 1, 3, and 4 the Ne-like (Ar^{8+}) line is stronger, due to the higher abundance of Ne-like ions at these times.

The analysis of the spectral data was done using a collisional-radiative model together with the HULLAC [12] atomic code. The atomic model used for calculating the Ne-like and F-like Ar ion configurations included 89 levels [13], providing sufficient accuracy. The levels' populations as well as the spectral lines' intensities were calculated in the electron density and temperature range relevant for the

compressed plasma column conditions ($T_e = 60\text{--}100$ eV, $N_e = 10^{18}\text{--}10^{20}$ cm^{-3}), assuming quasi-steady-state conditions and taking into account the measured cylindrical geometry of the plasma column.

Intensity ratios of Ne-like lines ($2p-3d$ and $2p-4d$ lines relative to the $2p-3s$ line) that are highly sensitive to the plasma temperature and density in this range were measured and compared to the calculated values [11]. For example, at 10^{20} cm^{-3} and 100 eV the calculated values are $I_{2p-3d}/I_{2p-3s} = 5.7$ and $I_{2p-4d}/I_{2p-3s} = 2.4$, whereas at 10^{19} cm^{-3} and 80 eV the calculated values are only $I_{2p-3d}/I_{2p-3s} = 1.7$ and $I_{2p-4d}/I_{2p-3s} = 0.6$. The measured line ratios in spectrum No. 2 (Fig. 3) are $I_{2p-3d}/I_{2p-3s} \cong 5$ and $I_{2p-4d}/I_{2p-3s} \cong 2$, indicating that the plasma conditions in this case are about 10^{20} cm^{-3} and 100 eV (i.e., unsuitable conditions for lasing in Ne-like Ar [5,6]). These results were confirmed by the calculations performed over the entire density and temperature range and also by other experimental evidence: First, the relatively strong $2p-3d$ line emission of the Ar^{9+} (F-like Ar) ion, which is about the same magnitude as the Ne-like Ar $2p-3d$ line, indicates a high electron temperature (>90 eV). Second, the observed intensity of the Ne-like Ar $2p-3d$ line ($\lambda = 41.48$ \AA) is comparable to the two adjacent $2p-3d$ lines. This line intensity, which is expected to be much stronger at moderate densities ($N_e < 10^{19}$ cm^{-3}), indicates that the electron density is high ($\geq 10^{20}$ cm^{-3}).

While repeating this analysis procedure for the other spectra we found that at the time the shock wave reaches the axis (spectrum No. 1, $t = 45$ ns), as well as at later times (spectra Nos. 3 and 4, $t = 64, 68$ ns), the plasma is colder and less dense, achieving the required electron density and temperature for lasing. However, two other

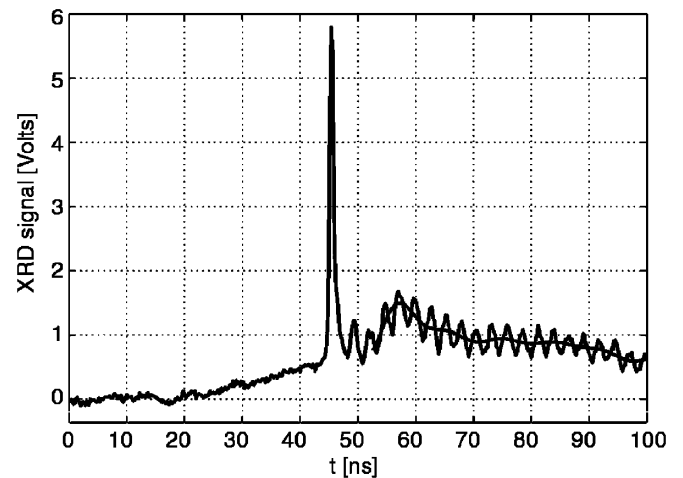


FIG. 4. Carbon x-ray diode signal showing the lasing action at $t = 45$ ns. The noisy signal seen afterwards appeared only in cases where strong lasing was detected. The maximum of the spontaneous emission appears at $t = 58$ ns according to the averaged line obtained by applying a low pass filter at later times ($t > 50$ ns).

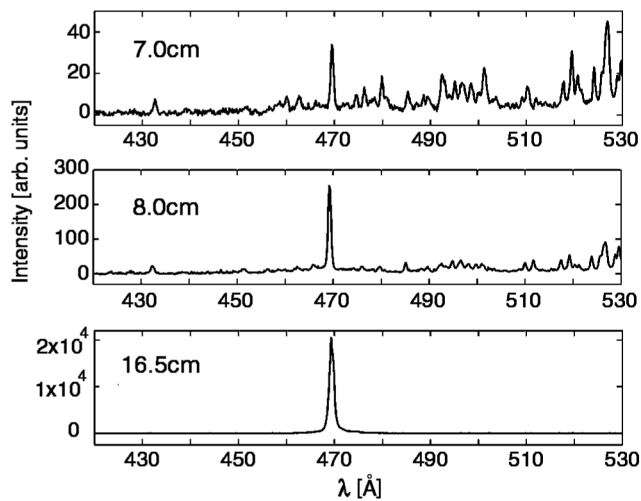


FIG. 5. Soft x-ray spectra in the 420–530 Å spectral range, while using $L = 7, 8,$ and 16.5 cm capillary lengths. Strong amplification of the 469 Å $3p \rightarrow 3s$ ($J = 0-1$) line is evident.

conditions are needed for soft x-ray laser realization: a concave electron density profile in the radial direction for achieving beam guiding [14,15] and a thin plasma diameter ($<100 \mu\text{m}$) for avoiding the self-absorption of the Ne-like Ar $2p-3s$ line [5]. These conditions are satisfied (according to the measured column radius presented in Fig. 2, as well as to our magnetohydrodynamic code results [16]) only in the first case ($t = 45$ ns).

A time dependent measurement of the soft x-ray radiation emitted from the capillary source (with $L = 16.5$ cm), obtained by an x-ray diode with a graphite cathode, at the same experimental conditions, is presented in Fig. 4. On top of the spontaneous emission signal that lasts for tens of nanoseconds, the laser signature is clearly seen, at the predicted time ($t = 45$ ns), as a sharp high amplitude pulse. The full width half maximum of the laser pulse is about 800 ps.

In order to measure the soft x-ray line amplification three spectra were taken while using different capillary lengths ($L = 7, 8, 16.5$ cm). These spectra, presented in Fig. 5, were obtained at $t = 45$ ns (3 ns exposure time) with a 300 l/mm grating adjusted to the 420–530 Å spectral range. The significant growth of the intensity of the Ne-like Ar $3p \rightarrow 3s$ ($J = 0-1$) line at 469 Å is clearly seen (we note that the spectrometer detector was partly saturated in the last measurement). The detected gain coefficient according to our x-ray diode measurements is $G > 0.75 \text{ cm}^{-1}$. The small divergence of this line seen on the spectrometer camera raw data (<5 mrad) is also a clear evidence of lasing.

In conclusion, detailed measurements of the plasma column dynamics, stability, electron density, and temperature were obtained in a capillary discharge experiment. These measured parameters allowed us to tune the initial conditions and the external parameters in order to achieve the

required conditions for soft x-ray amplification. Indeed, when the appropriate conditions were applied, strong amplification in a long and narrow plasma column was observed. The experimental methods described above may be used for soft x-ray lasers realization at even shorter wavelengths [17,18], where the usage of even higher current pulses will require an accurate control of the stability and the dynamics of the collapsing column.

This work was partially supported by the Fund for Encouragement of Research in the Technion. We acknowledge the assistance of U. Avni, S. Aricha, and Y. Erlich in implementing the soft x-ray laser experiment.

-
- [1] D. L. Matthews *et al.*, Phys. Rev. Lett. **54**, 110 (1985).
 - [2] S. Suckewer *et al.*, Phys. Rev. Lett. **55**, 1753 (1985).
 - [3] J. J. Rocca *et al.*, Phys. Rev. Lett. **73**, 2192 (1994).
 - [4] F. G. Tomasel, J. J. Rocca, V. N. Shlyaptsev, and C. D. Macchietto, Phys. Rev. A **55**, 1437 (1997).
 - [5] V. N. Shlyaptsev, J. J. Rocca, and A. L. Osterheld, Proc. SPIE Int. Soc. Opt. Eng. **2520**, 365 (1995).
 - [6] D. E. Kim, D. S. Kim, and A. L. Osterheld, J. Appl. Phys. **84**, 5862 (1998).
 - [7] A. Ben-Kish, M. Shuker, R. Nemirovsky, A. Ron, and J. L. Schwob, in *X-ray Lasers—1998, Proceedings of the 6th International Conference on X-ray Lasers*, edited by Y. Kato, H. Takuma, and H. Daido, IOP Conf. Proc. No. 159 (Institute of Physics and Physical Society, London, 1998), p. 191.
 - [8] A. Ben-Kish, R. Nemirovsky, M. Shuker, A. Ron, and J. L. Schwob, Proc. SPIE Int. Soc. Opt. Eng. **3776**, 166 (1999).
 - [9] A. Ben-Kish, M. Shuker, R. A. Nemirovsky, U. Avni, A. Fisher, A. Ron, and J. L. Schwob, in Proceedings of the 7th International Conference on X-ray Lasers, 2000 (to be published).
 - [10] J. L. Schwob, A. W. Wouters, S. Suckewer, and M. Finkenthal, Rev. Sci. Instrum. **58**, 1601 (1987).
 - [11] A. Ben-Kish, Ph.D. thesis, Technion, Haifa, Israel, 2000.
 - [12] A. Bar-Shalom, M. Klapisch, and W. H. Goldstein (unpublished).
 - [13] R. Doron, Hebrew University, Jerusalem, Israel (private communication).
 - [14] R. A. London, Phys. Fluids **31**, 184 (1987).
 - [15] J. L. A. Chilla and J. J. Rocca, J. Opt. Soc. Am. B **13**, 2841 (1996).
 - [16] R. A. Nemirovsky, A. Ben-Kish, M. Shuker, and A. Ron, in *BEAMS'98: Proceedings of the 12th International Conference on High-Power Particle Beams, Haifa, Israel, 1998*, edited by Meir Markovits and Joseph Shiloh (IEEE, Piscataway, NJ, 1998), p. 638; R. A. Nemirovsky, A. Ben-Kish, M. Shuker, and A. Ron, Phys. Rev. Lett. **82**, 3436 (1999).
 - [17] M. Shuker, A. Ben-kish, R. A. Nemirovsky, and A. Ron, in *X-ray Lasers—1998, Proceedings of the 6th International Conference on X-ray Lasers* (Ref. [7]), p. 187.
 - [18] M. Frati, F. G. Tomasel, B. Bowers, J. J. Gonzalez, V. N. Shlyaptsev, and J. J. Rocca, in Proceedings of the 7th International Conference on X-ray Lasers, 2000 (to be published).